ORGANIC LETTERS

2005
Vol. 7, No. 17
3693−3696

# Parity and Heteroatom Effects on Open-Shell Exchange Interactions: Nitrenophenyl Iminoylnitroxides

**Patrick Taylor, Paul R. Serwinski, and Paul M. Lahti***

*Department of Chemistry, University of Massachusetts, Amherst, Massachusetts 01003*
*lahti@chem.umass.edu*

**Received June 2, 2005**

## ABSTRACT

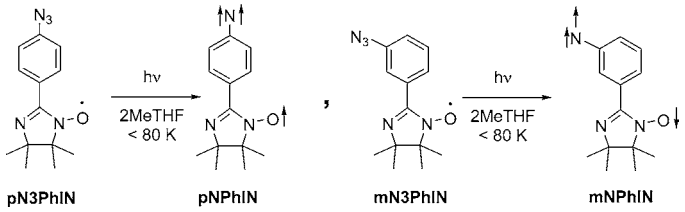


pN3PhIN pNPhIN mN3PhIN mNPhIN

**Photolysis of pN3PhIN and mN3PhIN in frozen matrix yields pNPhIN and mNPhIN, respectively. pNPhIN gives a quartet state with nonlinear ESR intensity behavior ($|D/hc| = 0.300$ cm$^{-1}$, $|E/hc| \cong 0.0$ cm$^{-1}$); mNPhIN gives a thermally excited quartet state ($|D/hc| = 0.336$ cm$^{-1}$, $|E/hc| = 0.006$ cm$^{-1}$) with inverse Curie behavior. Computations show little nitrene delocalization onto the radicals even for the para system. The NPhIN systems behave differently from analogous nitronylnitroxides due to asymmetric radical spin distribution.**

There is much interest in understanding interelectronic exchange interactions and ground-state spin multiplicity in conjugated molecules with multiple unpaired electrons. While qualitative parity-connectivity and spin-polarization models have been successful in predicting ground states for most conjugated non-Kekulé molecules,[1] heteroatom substitution can give unexpected[2] results. The magnitude and even sign of major exchange interactions can vary significantly in open-shell $\pi$-systems with different connectivities and heteroatom placement, due to changes in HOMO−LUMO gaps and spin density distributions.

We have described studies of nitreno radicals **pNPhNN** and **mNPhNN** under cryogenic matrix conditions.[3] Variable-temperature ESR and computational modeling indicate that **pNPhNN** has a high-spin quartet ground state, while **mNPhNN** has a low-spin doublet ground state.

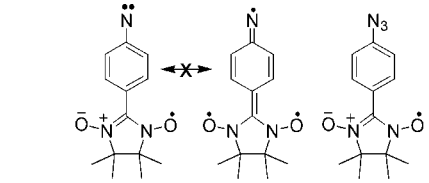

pNPhNN pNPhNN-Q pN3PhNN

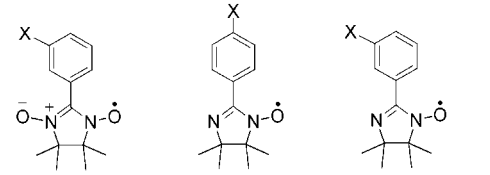

mNPhNN (X = N:) pNPhIN (X = N:) mNPhIN (X = N:)
mN3PhNN (X = $N_3$) pN3PhIN (X = $N_3$) mN3PhIN (X = $N_3$)

*m*-Phenylene linkage of unpaired electrons frequently gives ferromagnetic exchange of unpaired $\pi$-spins, but in **pNPhNN** para connectivity gives high-spin trimethylenemethane type exchange between the nitrenophenyl group (**NPh**) and the nitronylnitroxide (**NN**) radical. By comparison, **mNPhNN** has a pseudo-disjoint[1c] connectivity with spin−orbitals that can be localized on nonoverlapping atoms, with consequent

(1) (a) Ovchinnikov, A. A. *Theor. Chim. Acta* **1978**, *47*, 297. (b) Klein, D. J. *Pure Appl. Chem.* **1983**, *55*, 299. (c) Borden, W. T.; Davidson, E. R. *J. Am. Chem. Soc.* **1977**, *99*, 4587. (d) Cf. Lahti, P. M. In *Molecule-Based Magnetic Materials. Theory, Techniques, and Applications*; Turnbull, M. M., Sugimoto, T., Thompson, L. K., Eds.; American Chemical Society: Washington, DC, 1996; Vol. 644, pp 218−235.

(2) (a) Borden, W. T.; Iwamura, H.; Berson, J. A. *Acc. Chem. Res.* **1994**, *27*, 109. (b) Lahti, P. M. In *Molecule-Based Magnetic Materials. Theory, Techniques, and* Applications; Turnbull, M. M., Sugimoto, T., Thompson, L. K., Eds.; American Chemical Society: Washington, DC, 1996; Vol. 644, pp 218−235.

(3) (a) Lahti, P. M.; Serwinski, P. R.; Esat, B.; Liao, Y.; Walton, R.; Lan, J. *J. Org. Chem.* **2004**, *69*, 5247. (b) Lahti, P. M.; Esat, B.; Liao, Y.; Serwinski, P.; Lan, J.; Walton, R. *Polyhedron* **2001**, *20*, 1647.

10.1021/ol051295u CCC: $30.25 
**Published on Web 07/26/2005**

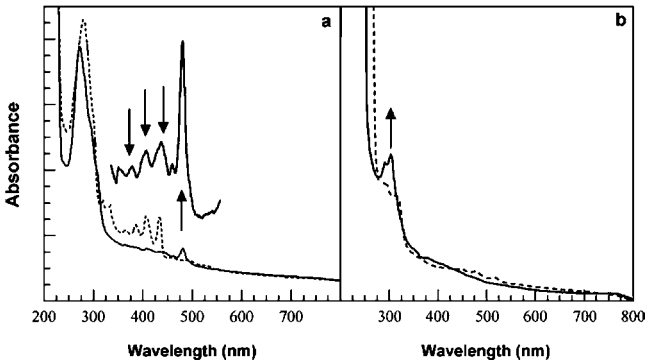


**Figure 1.** UV−vis spectra before (- - -) and after (—) frozen solution photolyses of diazides **pN3PhIN** (a, 18 K) and **mN3PhIN** (b, 15 K) in frozen 2-methyltetrahydrofuran. Peaks that decrease or increase after photolysis are shown with arrows.

limited exchange between the **NPh** group and the **NN**. ESR and computations suggest limited $\pi$-spin delocalization in both **NPhNN** systems, with **pNPhNN** being a nitreno radical rather than a delocalized quinonoidal triradical **pNPhNN-Q**.[3] In this paper, we describe a study of the related nitreno radicals **pNPhIN** and **mNPhIN** and differences caused by replacing the symmetrical **NN** radical with an iminoylnitroxide (**IN**) radical having an asymmetric spin distribution.

Precursor molecules **pN3PhIN** and **mN3PhIN** were synthesized by treatment of previously described[3] **pN3PhNN** and **mN3PhIN** with acidic aqueous $NaNO_2$ and column chromatography of the crude product. **pN3PhIN** is a readily isolable red solid, while **mN3PhIN** is a red oil. Both were characterized by solution ESR spectroscopy, analytical HPLC, and high-resolution mass spectrometry.

Photolysis of **pN3PhIN** and **mN3PhIN** in frozen 2-methyltetrahydrofuran shows little color change, unlike analogue **pN3PhNN**, which turns from blue to bright magenta. Precursor **pN3PhIN** has a major peak at 282 nm, a shoulder at 335 nm, and an apparent vibrational progression at 371, 391, 410, and 435 nm. After photolysis, the major peak shifts slightly to 274 nm, and a sharp new peak is produced at 483 nm (Figure 1) that is attributed to **pNPhIN**. **mN3PhIN** photolysis decreases the weak precursor peaks at 450−550 nm, with appearance of a weak absorption peak at about 300 nm attributed to **mNPhIN**. All peaks attributed to **pNPhIN** and **mNPhIN** disappear irreversibly upon softening the matrix above 90−100 K but do not change significantly over 14−80 K.

The 483 nm peak of **pNPhIN** is consistent with the para conjugation possible between nitrene and **IN** spin units and with donor−acceptor character such as that described by Shultz[4] for heterospin open-shell systems. TD-DFT/B3LYP/6-31G* computations with Gaussian 03 for both quartet and doublet states show a good match to a moderate intensity doublet-state transition at 490 nm.[5] The limited spectral change in **mNPhIN3** photolysis is consistent with a lack of direct **NPh** to **IN** $\pi$-conjugation in **mNPhIN** and with the TD-DFT computations showing only weak transitions above 400 nm for quartet or doublet.

(4) Shultz, D. A. *Polyhedron* **2003**, *22*, 2423.

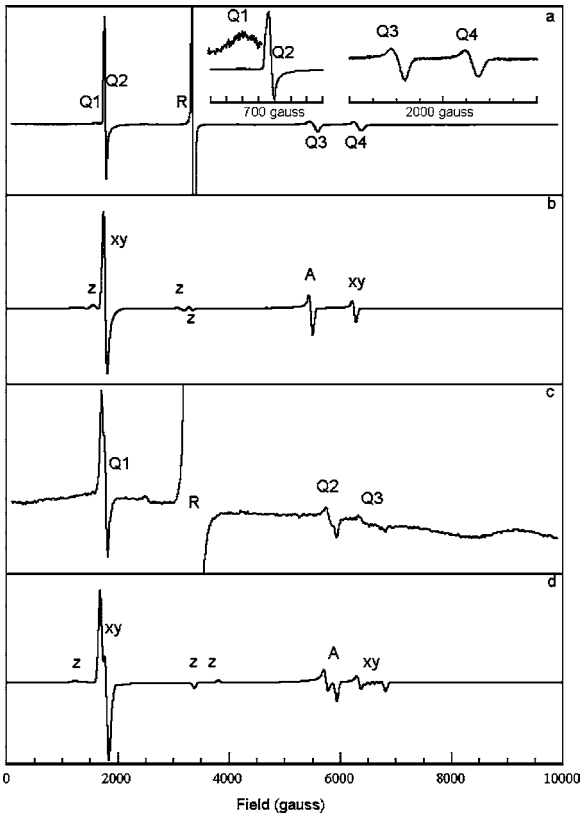


**Figure 2.** ESR spectra from photolyses of **pN3PhIN** (a, $\nu_0 = 9.454$ GHz, 77 K) and **mN3PhIN** (c, $\nu_0 = 9.373$ GHz, 90 K in MTHF, with comparison to eigenfield simulations (b,d). Q denotes quartet state peak, R denotes $S = 1/2$ state peak(s). (a) The Q1−Q2 inset region is from 1400 to 2100 G and the Q3−Q4 inset region is from 5000 to 7000 G.

ESR spectra obtained from frozen solution photolyses of **pN3PhNN** and **mN3PhNN** are shown in Figure 2. Peaks marked Q were obtained after brief irradiation of **pN3PhIN** at 77 or 4.2 K, at 1550 (weak), 1770 (strong), 5456, and 6250 G, plus a remnant 3340 G peak from unphotolyzed **pN3PhIN**. By comparison, 15 min photolysis of **mN3PhIN** at 4.2 K showed only the peak at about 3340 G. But, upon slow warming the photolyzed sample showed new peaks at 1785 (split), 5810, 5940, and ~6470 G (broad) that grew in intensity. The intensity changes for the spectra were reversible upon thermal cycling, with irreversible disappearance upon matrix thawing.

(5) Frisch, M. J.; Trucks, G. W.; Schlegel, H. B.; Scuseria, G. E.; Robb, M. A.; Cheeseman, J. R.; Montgomery, J. A. J.; Vreven, T.; Kudin, K. N.; Burant, J. C.; Millam, J. M.; Iyengar, S. S.; Tomasi, J.; Barone, V.; Mennucci, B.; Cossi, M.; Scalmani, G.; Rega, N.; Petersson, G. A.; Nakatsuji, H.; Hada, M.; Ehara, M.; Toyota, K.; Fukuda, R.; Hasegawa, J.; Ishida, M.; Nakajima, T.; Honda, Y.; Kitao, O.; Nakai, H.; Klene, M.; Li, X.; Knox, J. E.; Hratchian, H. P.; Cross, J. B.; Adamo, C.; Jaramillo, J.; Gomperts, R.; Stratmann, R. E.; Yazyev, O.; Austin, A. J.; Cammi, R.; Pomelli, C.; Ochterski, J. W.; Ayala, P. Y.; Morokuma, K.; Voth, G. A.; Salvador, P.; Dannenberg, J. J.; Zakrzewski, V. G.; Dapprich, S.; Daniels, A. D.; Strain, M. C.; Farkas, O.; Malick, D. K.; Rabuck, A. D.; Raghavachari, K.; Foresman, J. B.; Ortiz, J. V.; Cui, Q.; Baboul, A. G.; Clifford, S.; Cioslowski, J.; Stefanov, B. B.; Liu, G.; Liashenko, A.; Piskorz, P.; Komaromi, I.; Martin, R. L.; Fox, D. J.; Keith, T.; Al-Laham, M. A.; Peng, C. Y.; Nanayakkara, A.; Challacombe, M.; Gill, P. M. W.; Johnson, B.; Chen, W.; Wong, M. W.; Gonzalez, C.; Pople, J. A. *Gaussian 03*, B03 ed.; Gaussian, Inc.: Pittsburgh, PA, 2003.

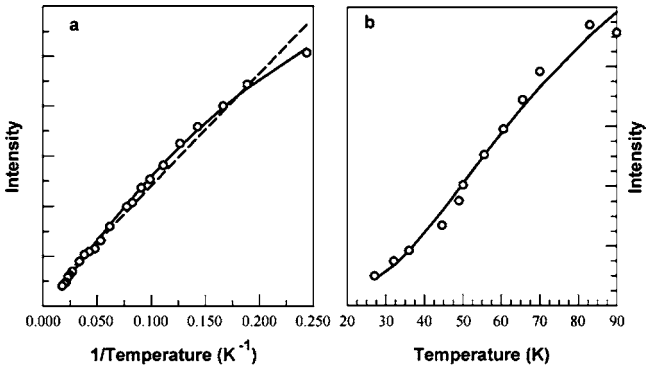


**Figure 3.** Curie plots for **pNPhIN** (1770 G peak, a) and **mNPhIN** (1785 G peak, b). The solid lines are fits to eq 1; the dashed line is a linear fit.

The "Q" peaks were attributed to quartet-state ESR transitions from **pNPhIN** and **mNPhIN** by their similarity to the spectra previously observed[3] for **pNPhNN** and **mNPhNN.** Line shape simulations using the eigenfield method[6] gave good fits to the observed spectra (Figure 2b,d) for $S = 3/2$ and $g = 2.003$; for **pNPhIN**, $|D/hc| = 0.300$ cm$^{-1}$, $|E/hc| < 0.002$ cm$^{-1}$; for **mNPhIN**, $|D/hc| = 0.336$ cm$^{-1}$, $|E/hc| = 0.006$ cm$^{-1}$.

Figure 3 shows thermal intensity variation for major peaks of the quartet ESR spectra. **pNPhIN** gave a slightly curved Curie plot consistent with a doublet below quartet state equilibrium (eq 1, $I(T)$ = peak intensity, $T$ = temperature) where $\Delta E(\mathrm{D}\rightarrow\mathrm{Q}) = 12.0 \pm 0.8$ cal/mol (uncertainty is the standard deviation). The small curvature could be due to saturation despite our use of low spectral power, although even a linear Curie plot may arise from nearly degenerate high and low spin states.[7] The TD-DFT computations for **pNPhIN** also support a doublet-quartet near degeneracy, since the predicted doublet transition matches the experimental UV−vis of Figure 1 better than any quartet transitions. By comparison, ESR Curie analysis and computations for **pNPhNN** supported[3a] a high-spin quartet ground state, and TD-DFT computations from this work predict that quartet **pNPhNN** has much stronger UV−vis transitions above 450 nm than the doublet state, in reasonable accord with the strong coloration[3a] of **pNPhNN**.

$$I(T) = \frac{4 \cdot e^{-\Delta E/RT}}{4 \cdot e^{-\Delta E/RT} + 2} \qquad (1)$$

By comparison, the **mNPhIN** quartet ESR peaks exhibited reversible inverse Curie intensity behavior in the range 25−70 K (Figure 3), attributable to a thermally populated state. Fitting of the intensity versus temperature data to eq 1 gave $\Delta E(\mathrm{D}\rightarrow\mathrm{Q}) = 266 \pm 21$ cal/mol.

(6) (a) Teki, Y. Ph.D. Dissertation, Osaka City University, Osaka, Japan, 1985. (b) Teki, Y.; Takui, T.; Yagi, H.; Itoh, K.; Iwamura, H. *J. Chem. Phys.* **1985**, *83*, 539. (c) Sato, K. Ph.D. Dissertation, Osaka City University, Osaka, Japan, 1994.

(7) See Berson, J. A. In *The Chemistry of Quinoid Compounds*; Patai, S., Rappaport, Z., Eds.; John Wiley and Sons: 1988; Vol. 2, pp 462−469.

**Scheme 1.** Qualitative Ground-State Spin Multiplicity Predictions for the **NPhNN** and **NPhIN** Systems

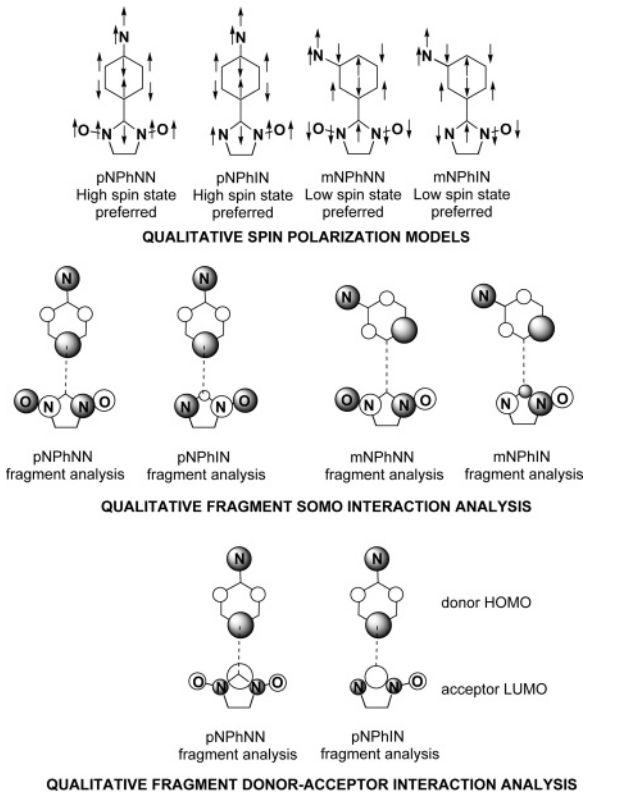


Various models can be used to explain the results for the **NPhINs** and compare them to the **NPhNNs**, as summarized in Scheme 1. For both **IN**- and **NN**-containing systems, para connectivity favors a high-spin quartet ground state, while meta connectivity favors a low-spin doublet state. Fragment analysis also suggests that high-spin stabilizing spin alternation will be better in **pNPhNN,** since para linkage of phenylnitrene to **NN** occurs at a nodal site, while a non-nodal site connection to asymmetric **IN** occurs in **pNPhIN**. **mNPhNN** has a pseudo-disjoint connection across fragment MO nodal sites, minimizing exchange interaction of spins between separate regions of the molecule. Inter-spin exchange is stronger in **mNPhIN** than in **mNPhNN** because of the inter-fragment connection in the former at a non-nodal site of the **IN** unit.

These analyses suggest that polarized spin alternation to give a high spin state will be better in **pNPhNN** than **pNPhIN**. Disjoint[1c] spin localization with consequent decrease of exchange strength will be favored in **mNPhNN** over **mNPhIN**. For this reason, a low spin state is more favorable in **mNPhIN** because it has more exchange to break degeneracy between the spin states and favor the doublet state. Experimentally, **pNPhNN** shows[3] linear ESR Curie behavior and computational results favoring a high spin state, while **pNPhIN** shows slight Curie curvature that is consistent with near degeneracy of high and low spin states. Conversely the ESR-estimated $\Delta E(\mathrm{D}\rightarrow\mathrm{Q})$ is significantly larger for **mNPhIN** than for **mNPhNN**[3] (266 vs 13−15 cal/mol, respectively). These results are consistent with the fragment MO analysis.

**Scheme 2.** Qualitative UB3LYP/6-31G* SOMOs for **mNPhNN** and **mNPhIN**

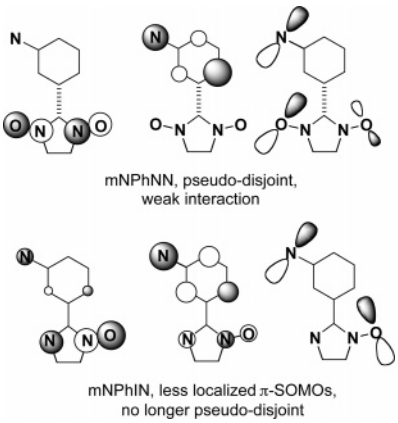


One may also use Shultz' donor−acceptor pardigm[4] for heterospin diradicals (Scheme 1) to analyze **NPhNN** versus **NPhIN** ground-state preferences. Stabilization is enhanced by small energy gaps between donor HOMO and acceptor LUMO, and by large HOMO/LUMO coefficients at the sites of connection between the donor and acceptor units. **IN** has a lower energy LUMO than **NN** for interactions with the same donor unit (phenylnitrene, in this case), which should strengthen the ferromagnetic (FM) donor−acceptor exchange term. **IN** has a smaller LUMO coefficient on the 2-carbon than **NN**, which will weaken its FM exchange term relative to **NN** with donors having the same connection parity. In the para systems, the stronger interaction between interacting coefficients should favor the donor−acceptor FM terms in **pNPhNN** over **pNPhIN**. This is consistent with the apparent greater favorability of the high spin state in **pNPhNN**. In the meta systems, the interplay of HOMO−LUMO gap and HOMO−LUMO coefficient interaction term is offsetting; the donor−acceptor model may not even apply so well here, since the UV−vis spectra of **mNPhNN** and **mNPhIN** do not show longer wavelength bands consistent with charge-transfer character.

To try to clarify the qualitative analyses of Scheme 1, we modeled the **NPhIN** systems with UB3LYP/6-31G* computations,[5] replacing methyl groups with C−H bonds. Bond lengths and Mulliken spin densities are given in supporting material. There is only a slightly smaller spin density on the nitreno nitrogen of **pNPhIN** by comparison to **mNPhIN** (1.58 versus 1.61), similar to the trends computed[3] for the corresponding **NPhNN** analogues. The nitrene site spin densities are virtually the same for the **NPhIN** and **NPhNN** systems, and for **NPh** itself. All the **NPhNN** and **NPhIN** systems are thus reasonably described as nitreno radicals, with little quinonoidal conjugation of nitrene spin density in the para isomers.

Scheme 2 qualitatively compares the UB3LYP/6-31G* SOMOs for **mNPhNN** and **mNPhIN**. In addition to the localized SOMO containing an n$\sigma$-type unpaired electron on the nitreno nitrogen, both systems have two $\pi$-SOMOs. The $\pi$-SOMOs are localized on the two different heterospin fragments in **mNPhNN**, consistent with its pseudo-disjoint character. But, the **mNPhIN** SOMOs both have contributions from both spin-bearing fragments, consistent with lesser spin localization and larger inter-fragment exchange expected from the Scheme 1 fragment analysis of **mNPhIN**. Spin density mismatches across the inter-ring connecting bonds of the $^2A_1$ state of **pNPhIN** and the $^4A$ state of **mNPhIN** raise their energies relative to the corresponding $^4A_1$ and $^2A$ states. The computations favor a quartet ground state in **pNPhIN** by 2.1 kcal/mol and a doublet ground state in **mNPhIN** by 0.7 kcal/mol. At the same level, **pNPhNN** favors a quartet by 6.3 kcal/mol, while **mNPhNN** favors a doublet by 1.5 cal/mol.[3a]

The computations show that spin density and SOMO coefficient distributions in the **NPhIN** and **NPhNN** systems follow the qualitative expectations of Scheme 1 and predict modest energy gaps between spin states, with the meta systems favoring low spin behavior. They do not properly reflect the experimentally smaller $^2A \rightarrow {}^4A$ gap in **mNPhNN** by comparison to **mNPhIN**, but given limitations[8] of density functional theory for estimating relative energies of multiconfigurational states with small energy gaps, we consider the computational findings to be reasonable.

An interesting conclusion of these studies is that *p*-phenylene connectivity from **NPh** to **NN** favors a high spin state, while the *m*-phenylene connectivity to either **NN** or **IN** favors a low spin state. This trend is opposite to that usually associated[9] with phenylene-linked diradicals, although violations are[10] known. In the case of the **NPhNNs** and **NPhINs**, the reversal of "normal" para/meta exchange parity occurs because of the spin density distributions in the **NN** and **IN** spin units, which effectively invert the parity from that expected when a large $\pi$-spin bearing atom is *directly* attached to a $\pi$-conjugated exchange linker unit (e.g., in *m*-benzoquinodimethane).

This work shows that heteroatom substitution in heterospin open-shell systems opens interesting and unusual possibilities for modulating exchange behavior and ground state spin multiplicity of non-Kekulé molecules. This should prove useful to workers interested in altering or even inverting the spin-parity expectations that apply to carbon-based open-shell $\pi$-conjugated systems.

**Acknowledgment.** This work was supported by the National Science Foundation (NSF CHE-0109094 and CHE-0415716). We are grateful to Prof. David Shultz for conversations that encouraged this study.

**Supporting Information Available:** Synthetic procedures, characterization, and computational summaries for **pN3PhIN** and **mN3PhIN**. This material is available free of charge via the Internet at http://pubs.acs.org.

OL051295U

(8) Cf, Davidson, E. R. *Int. J. Quantum Chem.* **1998**, *69*, 241.

(9) See the discussion by Borden, W. T. In *Magnetic Properties of Organic Materials*; Lahti, P. M., Ed.; Marcel Dekker: New York, 1999; p 61ff.

(10) (a) Borden, W. T.; Iwamura, H.; Berson, J. A. *Acc. Chem. Res.* **1994**, *27*, 109. (b) Fang, S.; Lee, M.-S.; Hrovat, D.; Borden, W. T. *J. Am. Chem. Soc.* **1995**, *117*, 6727.